TISSUE ENGINEERING: Part A
Volume 21, Numbers 7 and 8, 2015

DOI: 10.1089/ten.tea.2014.0280

# Chondrogenic Regeneration Using Bone Marrow Clots and a Porous Polycaprolactone-Hydroxyapatite Scaffold by Three-Dimensional Printing

Qingqiang Yao, MD, PhD,[1,2] Bo Wei, MD,[1] Nancy Liu, MD, PhD,[2] Chenshuang Li, DDS,[3,4] Yang Guo, MD,[1] Arya Nick Shamie, MD,[2] James Chen, MD,[2] Cheng Tang, MD, PhD,[1] Chengzhe Jin, MD, PhD,[1] Yan Xu, MD, PhD,[1] Xiuwu Bian, MD, PhD,[5] Xinli Zhang, MD, PhD,[3,5] and Liming Wang, MD[1]

Scaffolds play an important role in directing three-dimensional (3D) cartilage regeneration. Our recent study reported the potential advantages of bone marrow clots (MC) in promoting extracellular matrix (ECM) scaffold chondrogenic regeneration. The aim of this study is to build a new scaffold for MC, with improved characteristics in mechanics, shaping, and biodegradability, compared to our previous study. To address this issue, this study prepared a 3D porous polycaprolactone (PCL)-hydroxyapatite (HA) scaffold combined with MC (Group A), while the control group (Group B) utilized a bone marrow stem cell seeded PCL-HA scaffold. The results of *in vitro* cultures and *in vivo* implantation demonstrated that although an initial obstruction of nutrient exchange caused by large amounts of fibrin and erythrocytes led to a decrease in the ratio of live cells in Group A, these scaffolds also showed significant improvements in cell adhesion, proliferation, and chondrogenic differentiation with porous recanalization in the later culture, compared to Group B. After 4 weeks of *in vivo* implantation, Group A scaffolds have a superior performance in DNA content, Sox9 and RunX2 expression, cartilage lacuna-like cell and ECM accumulation, when compared to Group B. Furthermore, Group A scaffold size and mechanics were stable during *in vitro* and *in vivo* experiments, unlike the scaffolds in our previous study. Our results suggest that the combination with MC proved to be a highly efficient, reliable, and simple new method that improves the biological performance of 3D PCL-HA scaffold. The MC-PCL-HA scaffold is a candidate for future cartilage regeneration studies.

## Introduction

Due to the poor regenerative capacity of cartilage *in vivo*, articular cartilage defect is a great challenge in the field of orthopedic surgery.[1] There are several cartilage repair techniques, including microfracture, joint irrigation or debridement, osteochondral grafting, and autologous chondrocyte implantation.[2,3] As it is a simple, convenient, and relatively inexpensive choice, microfracture has become the preferred clinical treatment.[4] Previous evidence proved that bone marrow clots (MC) on the surface of the microfracture lesions provide an optimal environment for cartilaginous tissue repair.[5,6] However, this technique results in a repaired tissue with lower mechanical strength. This tissue is easily worn by daily activities, causing symptoms to recur and necessitating a second repair.[7,8] The poor mechanical strength, the instability of MC, and the loss of bone marrow-derived mesenchymal stem cell (BMSCs) may be the main barriers to fibrocartilage repair by microfracture.[9] Although the detailed mechanisms by which MC fibrocartilage forms are not clear, the combination of MC chondrogenic differentiation and high-strength biodegradable scaffolds may provide an advanced approach to the repair and functional reconstruction of cartilage defects.[10,11]

The fundamental concept underlying tissue engineering is the combination of a scaffold with living cells and/or biologically active molecules to form a ''tissue engineering construct'' that promotes the repair and/or regeneration of tissues.[12] Scaffolds, an essential element of three-dimensional (3D) cartilage construction, play important roles in directing cartilage regeneration. The components and structure of scaffolds determine their mechanical properties, biocompatibility,

[1]Department of Orthopaedic Surgery, Nanjing First Hospital, Nanjing Medical University, Nanjing, China.
[2]Department of Orthopaedic Research, David Geffen School of Medicine at University of California, Los Angeles, UCLA, Los Angeles, California.
[3]Dental and Craniofacial Research Institute, University of California, Los Angeles, UCLA, Los Angeles, California.
[4]Department of Orthodontics, School and Hospital of Stomatology at Peking University, Beijing, China.
[5]Institute of Pathology and Southwest Cancer Center, Southwest Hospital, Third Military Medical University, Chongqing, China.

and degradability, and thus inevitably influence the efficacy of 3D cartilage regeneration.[13,14] As shown by previous studies, natural, biodegradable materials including polylactic acid (PLA), polyglycolic acid (PGA), and PGA-PLA copolymer have good biocompatibility and biosafety.[15] However, poor mechanical strength and rapid degradability greatly limit their application in regenerating 3D tissue.[16] On the other hand, biomedical polymer materials have good mechanical strength and slow degradability, but poor biological effects.[17,18] As a semi-crystalline linear aliphatic polyester, polycaprolactone (PCL) is degraded by hydrolysis in physiological conditions and is now one of several degradable polymers the FDA has approved for use in the human body as a drug delivery device, adhesion barrier, and suture and staple. It is also being extensively investigated as a biomaterial for tissue repair and regeneration.[19] Currently, fused deposition modeling (FDM), an advanced rapid prototyping technique, can fabricate PCL/PCL-hydroxyapatite (HA) composites into a porous sponge or a honeycomb structure with designed shape.[17–20]

Furthermore, these porous structures may provide a network to mimic native extracellular matrix (ECM), which is favorable for cell adhesion and proliferation. The porous scaffold may also contain biological factors that promote cell proliferation and differentiation.[21,22] To improve the biological effects, numerous attempts have been set up to promote cell adhesion and ECM secretion of 3D PCL scaffolds by combining them with degradable bioactive materials (BMSC-derived natural ECM,[23,24] platelet-rich plasma,[26–28] and collagen[29]).

Our previous study testified that MC is able to regenerate cartilage by using biodegradable BMSC-derived ECM (BMSC-dECM) scaffolds. Furthermore, MC is easily obtained and has a rich content of BMSCs and biological factors.[8,23–25] The combination of PCL/PCL-HA scaffold and MC may be an effective approach to cartilage tissue engineering. However, whether the FDM 3D porous scaffold is suitable for MC in 3D cartilage regeneration is still unknown. Additionally, whether the collapse of MC-BMSC-dECM scaffolds can be improved by MC-PCL-HA scaffolds needs to be proved. To address these issues, this study prepared porous PCL-HA scaffolds by 3D FDM printing. We selected PCL-HA in accordance with a previous finding of cell adhesion and osteochondral histogenesis using the same materials.[30–32] The biomechanical strength and cartilage differentiation performance of the MC-PCL-HA scaffold, cultured *in vitro* and implanted *in vivo*, were examined to evaluate its suitability in cartilage regeneration.

## Materials and Methods

### *Animals*

For this study, 30 female New Zealand white rabbits (5–6 months old) and 60 female nude mice (6–7 weeks old) were used for BMSC isolation and microfracture and subcutaneous implantation models, respectively. The use of animals in this experiment was approved by the Institutional Animal Experiment Committee of Nanjing Medical University, and animals were treated according to the U.S. National Institutes of Health guidelines. All animals underwent veterinary examination to evaluate general health status. All experimental procedures, including bone marrow aspiration, microfracture, and subcutaneous dorsal implantation were performed under anesthesia.

### *BMSC isolation, culture, and identification with multi-directional differentiation*

Rabbit BMSCs were isolated and cultured as described in our previous study.[6,20,21] In brief, bone marrow was aspirated from the posterior superior iliac crest, and mononuclear cells (MNCs) were isolated by density gradient centrifugation. Cells were cultured in Dulbecco's modified Eagle's medium (DMEM; Gibco) supplemented with 10% fetal bovine serum (FBS; Gibco), 1% HEPES buffer, and 1% antibiotics-antimycotics in a 37°C, 5% $CO_2$ incubator. After primary cell expansion, osteoblastic, chondrogenic, and adipogenic differentiation were tested to confirm the identity of BMSCs using standard protocols[8] (Fig. 1).

### *Preparation of 3D porous scaffolds and grouping*

PCL-HA scaffolds were fabricated by FDM as previously described.[31–33] In brief, 3D PCL-HA porous scaffolds were designed by computer-aided design (CAD) in Geomagic studio 11.0 software. The structural parameters of the scaffolds were designed 8 mm in diameter, 1.5 mm in thickness, 100% pore interconnectivity, 700 μm fiber diameter with 0°/90° laydown pattern, 700 μm pore size, and 56% scaffold porosity.[18,21] PCL powder (molecular weight ~60,000; 3Dbiotek) and HA (Plasma Biotal) were dried separately for 24 h in a vacuum oven at 120°C and 40°C, respectively. The scaffolds were fabricated with PCL/30% HA (by weight) composite using 3D FDM microfabrication technology (FDM 3000 System; Stratasys, Inc.) following the manufacturer's protocol. All used chemicals were of pharmacological grade, and the detailed characterizations of these materials have been reported elsewhere.[34–36]

Two groups were set in this study: a PCL-HA combined with MC (Group A) and a BMSC inoculated PCL-HA scaffold as the control (Group B). Each group had 30 scaffolds, which were trimmed to a square of 6 mm × (4–6) mm in size for the *in vitro* experiment in an attempt to reduce deviations caused by small, uneven openings along the periphery. The two groups of *in vivo* scaffolds were subcutaneously implanted into the back of nude mice after 4 weeks of *in vitro* culture, and the mice were sacrificed at 4 weeks post-implantation. Scaffolds were sampled at day 1 and at weeks 1, 2, and 4 of *in vitro* culture, and at weeks 2 and 4 of *in vivo* implantation. Five samples were tested at each time point for each group ($n = 5$) (Fig. 1).

### *Preparation of MC-PCL-HA scaffold*

The microfracture procedure was performed bilaterally on the condyle of distal femurs in rabbit following the protocol in our previous study.[8,25] Each PCL-HA scaffold in Group A was immersed and mixed in MC retrieved from one rabbit, for 1 h, until the MC and scaffold were fully combined. Thirty MC/PCL-HA combined constructs were obtained. The amount of seeded stem cells was calculated as the difference between the stem cells in MNCs before and after the PCL-HA scaffold was immersed in the MC. In this study, the average $0.9 \pm 0.3 \times 10^5$ stem cells were loaded in each MC-PCL-HA scaffold.[32] These scaffolds were cultured in L-DMEM medium for 4 days, with the medium changed every 1–2 days until clear. Then, the MC-PCL-HA scaffolds were cultured in chondrogenic medium containing high-glucose DMEM, 10% FBS, 1% penicillin-streptomycin, 37.5 μg/mL L-ascorbic

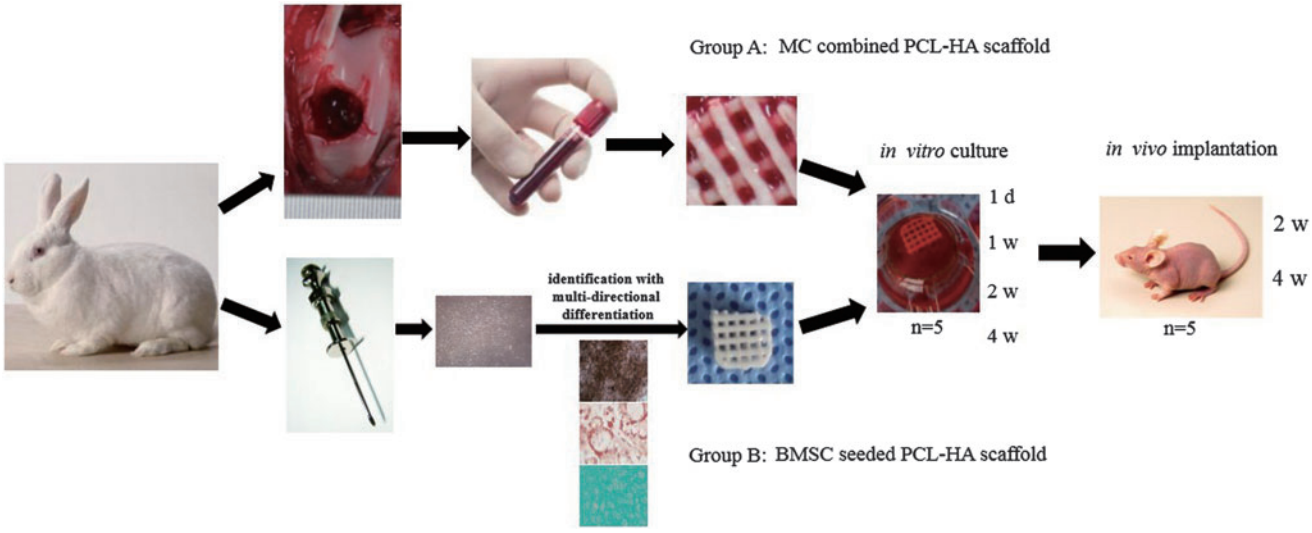


**FIG. 1.** Marrow clot (MC) combined polycaprolactone-hydroxyapatite (PCL-HA) scaffold and bone marrow-derived mesenchymal stem cells (BMSCs) seeded scaffold construction and grouping. The experimental details are described in the Materials and Methods section. Five samples were sampled at 1 day, and 1, 2, and 4 week time points for *in vitro* culture and 2, 4 week time points for *in vivo* implantation ($n=5$). Color images available online at www.liebertpub.com/tea

acid 2-phosphate, 40 μg/mL L-proline, 100 μg/mL sodium pyruvate, 6.25 μg/mL of recombinant human insulin, 6.25 μg/mL transferrin, 6.25 μg/mL selenous acid, 5.33 μg/mL linoleic acid, 10 ng/mL transforming growth factor-beta 3 (TGF-β3), and 100 nM dexamethasone (Pepro Tech) for 28 days *in vitro*, and then implanted in the dorsal subcutaneous tissue of nude mice for an additional 28 days. Each construct was implanted into one nude mouse. Scaffolds were sampled at day 1 and at weeks 1, 2, and 4 of *in vitro* culture, and at weeks 2 and 4 of *in vivo* implantation. Five samples were tested at each time point for each group ($n=5$) with 10 nude mice for *in vivo* implantation. This scaffold was designated as Group A.

### *Preparation of BMSC-seeded PCL-HA scaffolds*

A third passage of BMSCs were obtained and seeded onto tailored PCL-HA scaffolds with a density of $5\times10^5$/mL and a volume of 2 mL. Because the actual volume taken by each scaffold was similar to MC group ($0.3\pm0.1$ mL), the average $1–2\times10^5$ of BMSCs were loaded onto BMSC-PCL-HA scaffold. That was nearly equal to more than the amount of stem cells loaded in each MC-PCL-HA scaffold. After 1 h, the BMSC-seeded scaffolds were cultured in L-DMEM medium for 4 days with the medium changed every 2 days. Then, they were cultured in the chondrogenic medium (Cyagen Biosciences) for 28 days *in vitro* and implanted in the dorsal subcutaneous tissue of nude mice for an additional 28 days as described for the MC-PCL-HA scaffold. This scaffold type was designated as Group B.

### *Macro and microstructure morphology observation*

The macrostructure morphology of cultured 3D constructs was observed after 1 day and 1, 2, and 4 weeks of *in vitro* culture, and at 2 and 4 weeks postimplantation. Size, color, and shape were recorded. For pore morphology observations, an inverted microscope was used to identify the change of pore contents. For microstructure morphology observations, specimens were fixed in 10% formalin overnight, and then dehydrated through a series of graded ethanol solutions. Next, the samples were dried overnight at room temperature, gold sputtered, and observed by scanning electron microscope (SEM) (Jeol) at an accelerating voltage of 5 keV. Cell viability was assessed using Live/Dead Reduced Biohazard Viability/Cytotoxicity Kit (Molecular Probes) as per the manufacturer's protocol. Samples were washed with phosphate-buffered saline (PBS) and incubated in the dilute dye solution for 15 min at room temperature. Next, these samples were fixed with 4% glutaraldehyde for 1 h, and observed and photographed using a confocal microscope (Leica TCS SP2 Confocal Microscope; Leica). Live cells were stained green, and dead cells appeared red.

### *Mechanical testing*

Mechanical testing of specimens was conducted using Instron 4502 uniaxial testing system (Instron Ltd.). Scaffolds at 1, 2, and 4 weeks *in vitro*, and at 2 and 4 weeks *in vivo* underwent a single 1 mm/min compression until 10% strain was reached. Compression testing was also carried out under simulated physiological conditions by keeping the scaffolds at 37°C in PBS for 24 h before testing. The compressive strength of five scaffolds for each group was recorded at 10% strain with mean ± standard deviation calculated.

### *Histology and immunohistochemical staining assay*

Cultured tissue samples were fixed in 10% formalin for 24 h, dehydrated with a graded ethanol series, and embedded in paraffin wax. Sections were separately stained with Safranin O/Fast Green (SO-FG) and Hematoxylin-Eosin stain. After deparrafinizing samples and antigen retrieval, type II collagen immunohistochemical staining was performed using mouse anti-rabbit collagen type II monoclonal antibody (1:200 dilution; Novus Biological) and anti-mouse secondary antibody (1:200 dilution) (DakoCytomation). Then, samples

were incubated in 3,3′-diaminobenzidine tetrahydrichloride and counterstained with Mayer's hematoxylin (Sigma).

### *Biochemical measurement*

The content of type II collagen in engineered tissues was quantified by ELISA as previously described.[6,19] The sulfated glycosaminoglycan (GAG) content of engineered tissues was quantified by ELISA using dimethylmethylene blue (DMMB; Sigma Aldrich) colorimetric assay with chondroitin sulfate from shark cartilage to generate a standard curve. Total DNA content was measured using Quit-iT dsDNA kit (Invitrogen) with salmon test DNA to generate a standard curve. As the control group, the content of type II collagen, GAG, and total DNA in the native cartilage was measured using samples 6 mm in diameter and 2–3 mm in thickness.

### *Real-time PCR analysis*

Real-time PCR analysis was performed as previously described.[6,21] In summary, the specimens were rinsed twice with PBS buffer and lysed in TRIzol (Invitrogen). Total RNA was isolated and reverse transcribed to cDNA using High-capacity cDNA Reverse Transcription kit (Applied Biosystem). Real-Time PCR was performed with 40 cycles running for glyceraldehyde-3-phosphate dehydrogenase (GAPDH), type II collagen, Sox9, and Aggrecan using ABI Prism 7500 sequence detection system (Applied Biosystem), as per the manufacturer's protocol. The mRNA level of each gene was normalized to GAPDH and then compared with levels in the 1 week *in vitro* culture. Relative quantitation of gene expression was determined by standard $2^{(-\Delta\Delta Ct)}$ calculations. The primer sequences were designed using Primer 5 software, which are listed in Table 1.

### *Statistical analysis*

The statistical analysis was performed with SPSS 13.0 statistical software (SPSS, Inc.). All of the statistical analyses were performed using one-way analysis of variance (ANOVA). An unpaired Student's *t*-test was used to compare the differences in volume, biochemical composition content, and gene expression between Group A and Group B. A value of $p < 0.05$ was considered to be statistically significant. Data were tested for normality before performing the Student's *t*-test.

Table 1. Detailed Information of the Primer Sequences for RT-PCR

| *Gene* | *Primer nucleotide sequence* |
|---|---|
| GAPDH | Forward: 5-TCACCATCTTCCAGGAG CGA-3<br>Reverse: 3-CACAATGCCGAAGTGG TCGT-5 |
| Type II collagen | Forward: 5-GGCAATAGCAGGTTCACG TACA-3<br>Reverse: 3-TTCACCCCGTTCTGACAA TAGC-5 |
| Sox9 | Forward: 5-CACACAGCTCACTCGA CCTTG-3<br>Reverse: 3-GCTCTACTAGGATTTTATT GGCTT-5 |
| Aggrecan | Forward: 5-TCGAGGACAGCGAGGCC-3<br>Reverse: 3-AGAGATGTGCGATGTG GGAGCT-5 |

## Results

### *Observation of macro and microstructure of the scaffold*

The obtained PCL-HA scaffolds matched the design parameters in CAD, including size, shape, pore size and interconnectivity, and fiber diameter (Fig. 2). After replacing the medium of the 2 weeks *in vitro* culture, most erythrocytes on the MC-PCL-HA scaffold were washed off, thus reducing the red color of the scaffold. The size of each scaffold did not significantly change during *in vitro* culture, and no significant shrinkage was found after *in vivo* implantation for both groups (Fig. 3A). As time progressed, pore content accumulation was seen in Group B. In Group A, the density of content significantly decreased during the first week of *in vitro* culture, which was subsequently increased after the following culture (Fig. 3B). SEM analysis revealed that pores of scaffolds were filled and obstructed by fibrin, monocytes, and erythrocytes from MC at time point day 1, but they were gradually recanalized over the next 2 weeks. Similarly, the exogenous fibrin in Group B was removed after 1 week *in vitro* culture. Compared to Group B, more cells and ECM were accumulated inside the 3D porous framework of Group A during culture. No obvious changes in color were found in Group B during the first 2 weeks in culture; however, a slow and gradual accumulation of cells and ECM could still be found using SEM and inverted microscope (Fig. 3B). Specimens with smooth and shiny surfaces gradually formed in Group A after implantation, and they more closely displayed cartilage-like macro morphology than those in Group B (Fig. 3A). The confocal images of Live/Dead assay showed that red-stained dead cells in MC-PCL-HA scaffold were increased at the 1 week *in vitro* time point, and decreased at the 2 week *in vitro* culture time point. The pore obstruction and recanalization could also be observed in confocal images. However, rare red-stained dead cells were observed in Group B, with the density of adhered cells significantly lower during the first 2 weeks of *in vitro* culture (Fig. 4).

### *Mechanical test*

The mechanical property of both two groups gradually decreased during *in vitro* culture and increased during *in vivo* culture. For Group A, the mechanics at the 4 week time point for *in vitro* culture ($3.70 \pm 0.44$ MPa) was significantly lower than at the 1 day *in vitro* ($4.21 \pm 0.19$ MPa) ($p < 0.05$) and 4 weeks *in vivo* ($4.22 \pm 0.29$ MPa) ($p < 0.05$) time points. However, no apparent difference was found between the other two time points. Similarly, significant differences in mechanics were only found at the 4 weeks *in vitro* time point compared to day 1 ($3.52 \pm 0.28$ MPa, $4.23 \pm 0.18$ MPa, $p < 0.05$) and 4 weeks *in vivo* time point ($3.52 \pm 0.28$ MPa, $4.05 \pm 0.37$ MPa, $p < 0.05$) in Group B. The mechanics of samples in Group A was higher than Group B at the 1 and 2 week *in vitro* time points and 4 week time point for *in vivo* culture, but no statistical difference

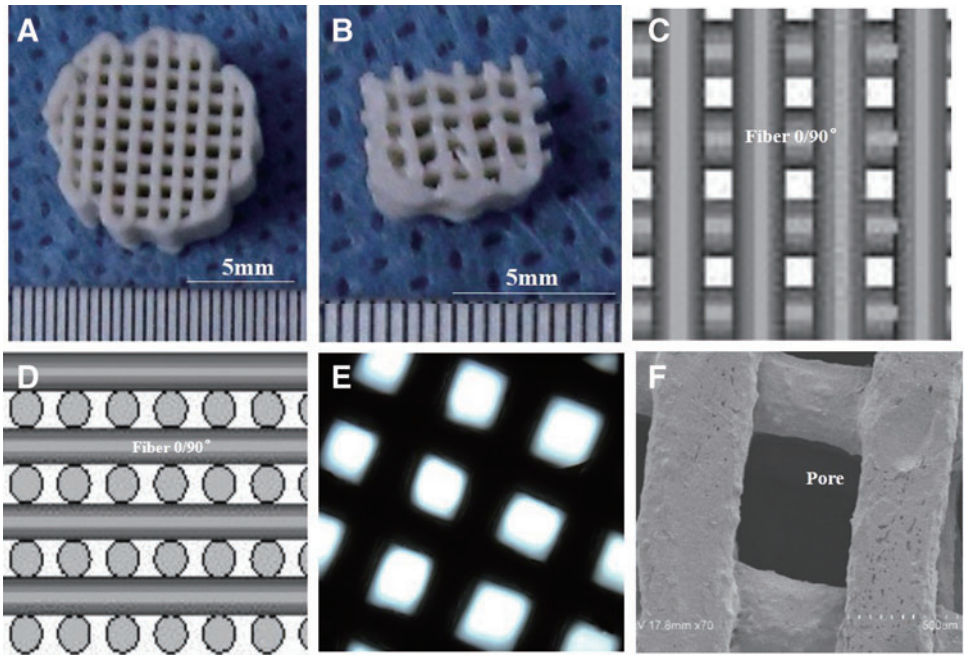


**FIG. 2.** Manufacturing of a three-dimensional (3D) PCL-HA porous scaffold. The details of scaffold design and preparation are described in the Materials and Methods section. The primary scaffold **(A)** was trimmed to a square **(B)** to reduce deviations caused by uneven, small openings along the periphery. The 3D fiber porous structure as shown by computer-aided design **(C, D)** matches the inverted microscope **(E)** and scanning electron microscope (SEM) **(F)** observations. Color images available online at www.liebertpub.com/tea

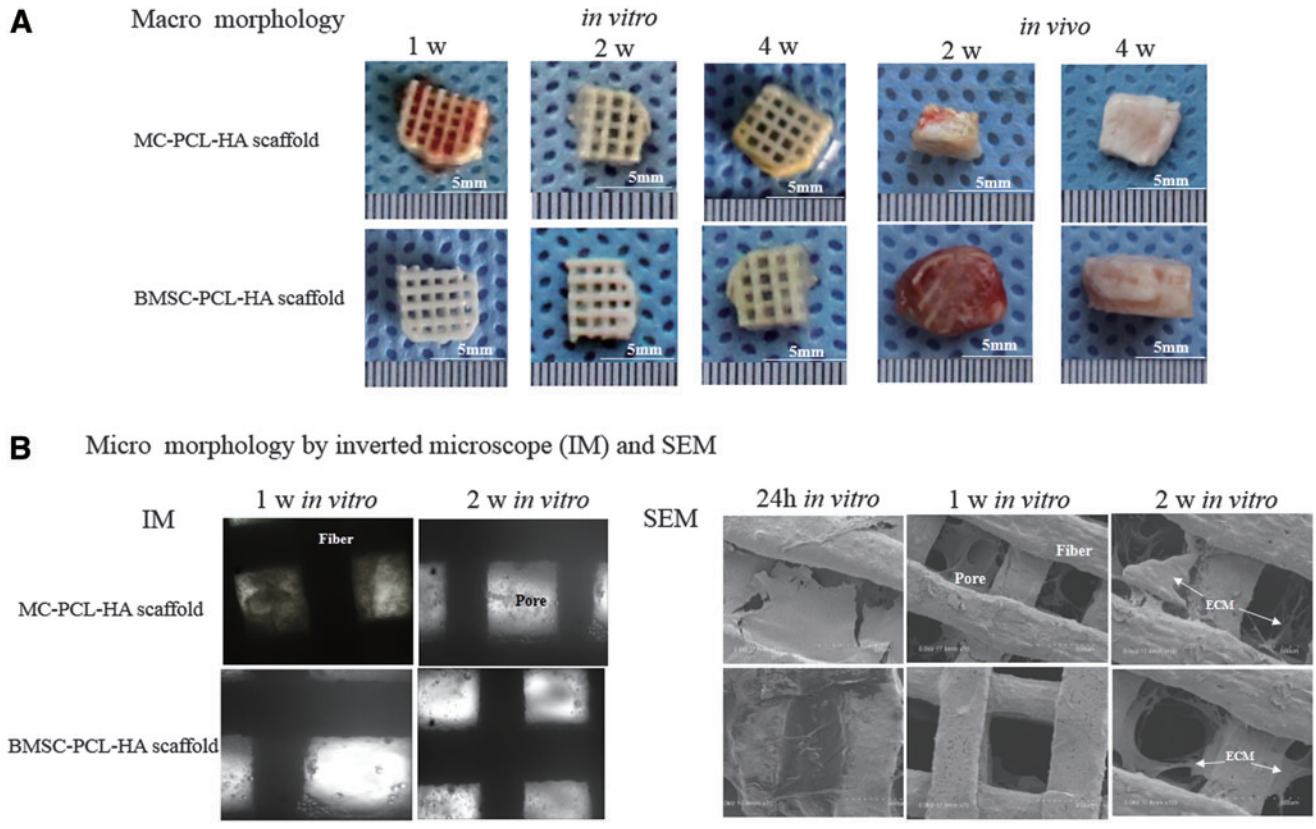


**FIG. 3.** Macro and micromorphology of cultured or implanted scaffolds. **(A)** For Group A, *in vitro* macromorphology showed that at early time points, the *red* color was gradually replaced by a yellowish appearance, while the matrix in the pore was seen accumulated in both groups. After *in vivo* implantation, cartilage-like appearance was found in Group A samples. No significant shrinkage was observed during *in vitro* and *in vivo* cultures for either group as compared to the corresponding initial implants. **(B)** The obstruction and recanalization of pores in Group A were observed during the first 2 weeks of *in vitro* culture. SEM confirmed a greater amount of matrix contents inside the pores of Group A, as compared to Group B, at the 1 and 2 week time points of *in vitro* culture. Color images available online at www.liebertpub.com/tea

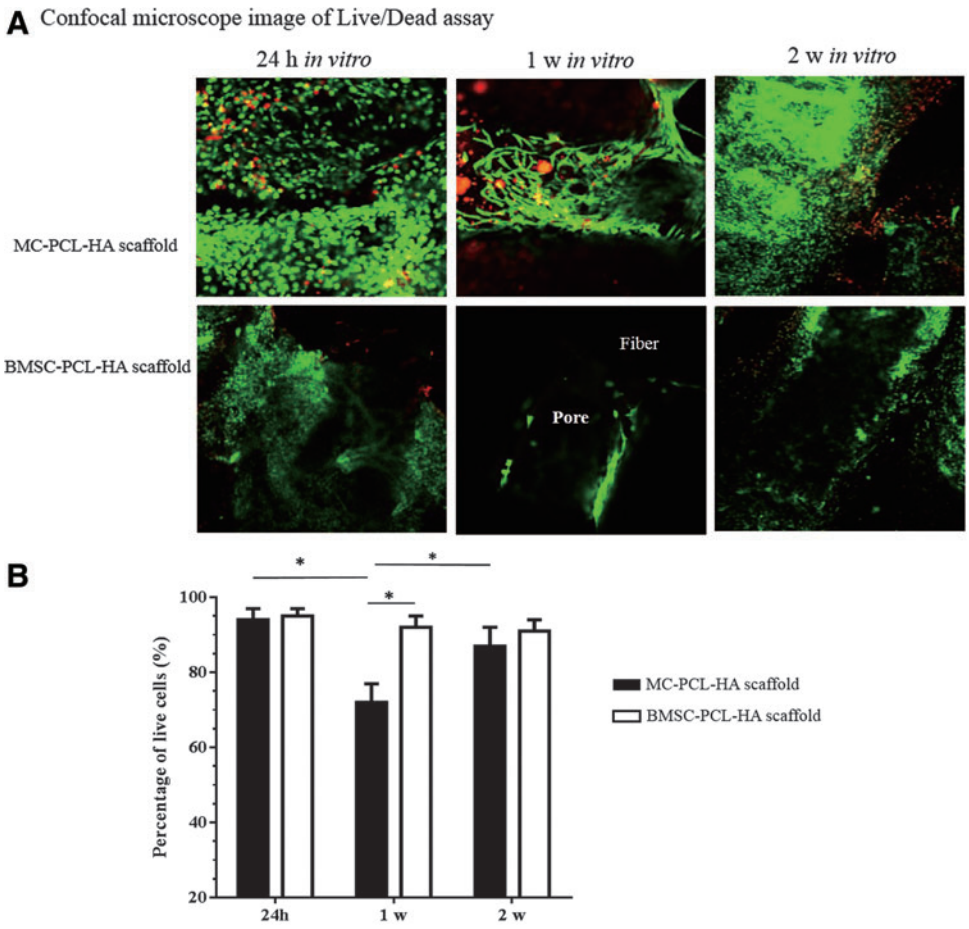


**FIG. 4.** Live/Dead assay of loaded stem cells. **(A)** The assay showed a greater amount of cells inside the MC-PCL-HA scaffolds, compared to BMSC-seeded scaffolds, during the first 2 weeks of culture, with more red-stained dead cell observed in MC-PCL-HA scaffolds. **(B)** The ratio of live/dead cells in Group A decreased at 1 week and increased at 2 weeks *in vitro* culture, and this ratio in Group A was lower than that of Group B. $*p < 0.05$. Color images available online at www.liebertpub.com/tea

was found between the two groups at each time point. The mechanics of the two groups was significantly higher than our previous BMSC-dECM scaffolds (0.5–1.8KPa during *in vitro* culture)[6,19–21] (Fig. 5).

### *Histology and immunohistochemical staining assay*

Histological analyses showed a larger amount of cartilage-like lacunas containing proliferated cells inside pores in Group A, at the 4 week *in vivo* implantation time point compared to Group B (Fig. 6 A, B, G, H). Meanwhile, SO-FG staining demonstrated that more GAG was synthesized and had accumulated inside the porous framework in Group A, while a smaller amount of GAG accumulation was found in Group B, at the 4 week time point for *in vivo* implantation (Fig. 6C, D, I, J). Similarly, immunohistochemical staining demonstrated an apparent synthesis and accumulation of higher levels of type II collagen in Group A at the 4 week time-point for *in vivo* samples, compared to samples at the same time point in Group B (Fig. 6E, F, K, L).

### *Analysis of biochemical components*

The quantitative measure of the collagen content showed that type II collagen, in both Group A and B, gradually increased as culture time progressed. Compared to Group B, tissues in Group A accumulated a larger amount, *in vitro*, from 1 week and on, with the most apparent difference observed at the *in vitro* 4 week time point ($227.1 \pm 21.4$ μg/mg, $160.4 \pm 18.7$ μg/mg,

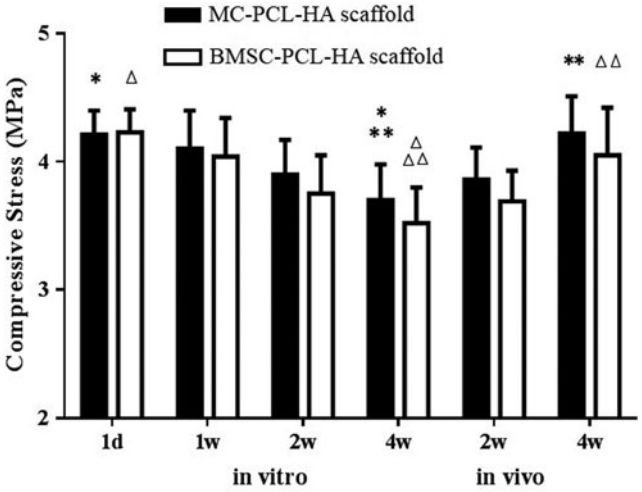


**FIG. 5.** The mechanical properties of both groups decreased gradually during *in vitro* culture, and it increased during *in vivo* implantation. The mechanics at the 4 week *in vitro* culture time point was significantly lower than the 1 day *in vitro* and 4 week *in vivo* time points in both groups. No apparent differences were found between other two time points. The mechanics for Group A samples was slightly higher than those of Group B at the 1 and 2 week *in vitro* culture time points, as well as 2 and 4 weeks after *in vivo* implantation. However, no statistical difference was found between the two groups at each time point. *, **, Δ, ΔΔ, $p < 0.05$.

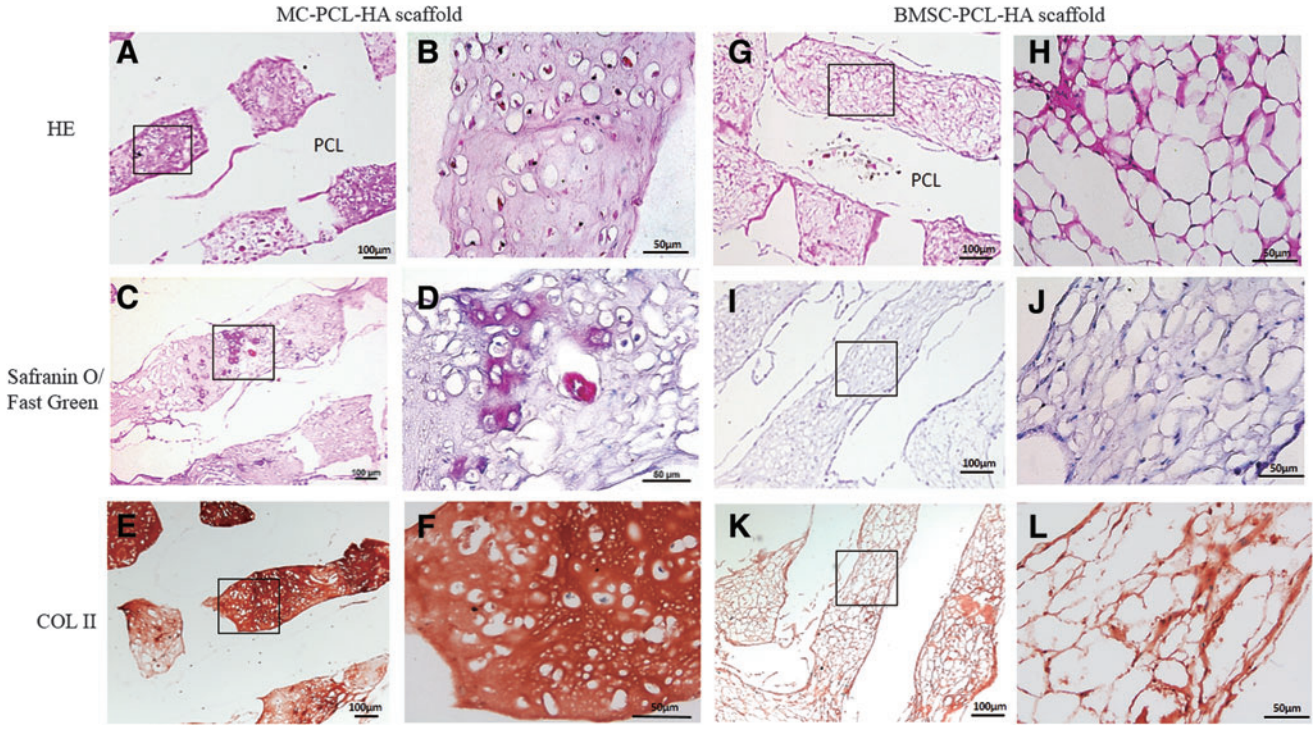


**FIG. 6.** Histological evaluation of implanted scaffolds with stem cells. Hematoxylin-Eosin (HE) staining **(A, B, G, H)**, Safranin O staining **(C, D, I, J)** and immunohistochemical staining with anti-collagen type II antibody (COL II) **(E, F, K, L)** of tissues in both the MC-PCL-HA and BMSC-seeded PCL-HA groups after 4 weeks *in vivo* implantation was performed. The results of glycosaminoglycan (GAG) and COL II staining, along with cartilage-like lacunas containing cell appearance demonstrated that the MC-PCL-HA scaffolds have a stronger capacity for chondrogenic differentiation compared to BMSC-seeded PCL-HA scaffolds. Black box: detailed magnification. Color images available online at www.liebertpub.com/tea

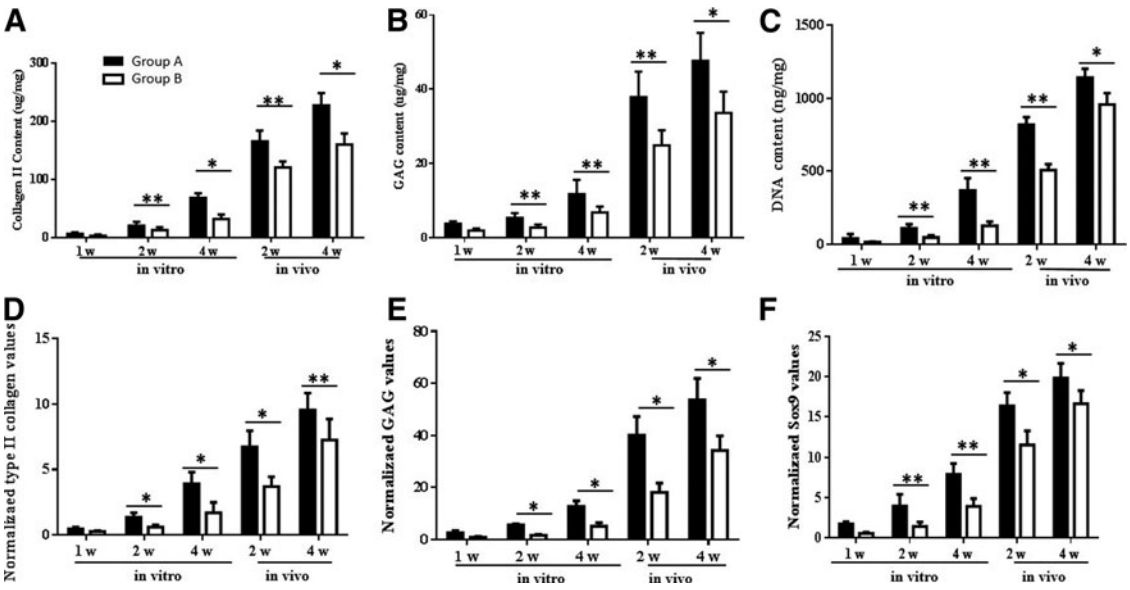


**FIG. 7.** Biochemical and gene expression assays of cultured tissues. The content and variation of collagen II **(A)**, GAG **(B)**, and DNA **(C)** were measured quantitatively during the culture period as described in the Materials and Methods section. MC combined PCL-HA scaffolds had a larger amount of Collagen II, GAG, and DNA accumulation than the BMSC-seeded PCL-HA scaffolds. The gene expression levels of collagen II **(D)**, GAG **(E)**, and SOX9 **(F)** was normalized to the housekeeping gene glyceraldehyde-3-phosphate dehydrogenase (GAPDH) and compared to the 1 week *in vitro* culture time point. Similarly, the expression of collagen II, GAG, and SOX9 in MC-PCL-HA scaffolds were higher than in BMSC seeded scaffolds during culture. $*p < 0.05$, $**p < 0.01$.

$p < 0.05$) (Fig. 7A). Similarly, the GAG content of both Group A and B gradually increased. The GAG content of Group A was notably higher than Group B at each time point, particularly for the peak value, which was found at the 4 week time point *in vivo* implantation ($47.63 \pm 7.61$ μg/mg, $33.61 \pm 5.73$ μg/mg, $p < 0.05$) (Fig. 7B). However, the DNA content of the two groups showed more rapid accumulation during the first 2 weeks *in vivo* implantation, when compared to the *in vitro* culture. At each time point, the DNA content in Group A was higher than Group B, with the difference between the two groups reaching a peak at 2 weeks *in vivo* ($818.2 \pm 52.5$ ng/mg, $508.4 \pm 40.3$ ng/mg, $p < 0.05$) (Fig. 7C).

### *Gene expression analysis*

The real-time PCR assay demonstrated that the expression of type II collagen in both Group A and B gradually increased during *in vitro* culture and after *in vivo* implantation, with the level of type II collagen expression in Group A significantly higher than Group B (Fig. 7D). The expression of GAG and Sox9 showed a similar trend in the two groups during *in vitro* culture and after *in vivo* implantation (Fig. 7E, F).

## Discussion

The specific structural, biomechanical, and biochemical characteristics of cartilaginous tissue has made cartilage tissue engineering a potentially valuable tool for the repair of cartilage defects.[1,2] In recent years, much attention has been focused on achieving cartilage regeneration by combining microfracture and scaffold materials (e.g., fibrin, hydrogel, and gelatin).[37,38] In our previous studies,[23–25] BMSC-dECM scaffolds had excellent effects on stem cell proliferation and chondrogenic differentiation in natural, biodegradable materials, especially when combined with MC. However, similar to other biological materials, the clinical usage of ECM scaffolds may be limited because of the poor mechanical strength and rapid biodegradability.[8,24] Biomedical polymer materials, with potentially better mechanic, shaping, and biodegradable characteristics, can be utilized to construct a porous scaffold with a specified shape and internal structure for the personalized and precise repair of damaged tissue.[17,18,21,39] Although the mechanics of the scaffolds in Groups A and B decreased after 4 weeks of *in vitro* culture and increased 4 weeks postimplantation due to the compounding effects from both competitive positive and negative forces, the mechanics of the MC-PCL-HA scaffold was notably higher and more stable than the natural biodegradable materials previously described.[20,23–25,40,41] Notably, there were no significant differences in mechanics between the MC combined scaffolds and the BMSC seeded scaffolds during *in vitro* culture and after *in vivo* implantation. It shows that using MC will not negatively impact the mechanics of the PCL-HA scaffold.

In this study, no significant shape shrinkage of the MC-PCL-HA scaffold was found during culture in comparison to their initial size at implantation. It has been reported that plasma contraction may lead to nearly 50% shrinkage of the MC-based scaffold. Similarly, studies, including our previous one, found that the tissue generated by MC will begin its shrinkage at 1 week after *in vitro* culture, and will completely disappear with poor cell proliferation and insufficient ECM secretion.[9,10] In this study, the macro morphology of the MC-PCL-HA scaffold maintained its shape throughout the experiments with the shrinkage of MC observed inside the pores of scaffold. This demonstrated that the PCL-HA scaffold can significantly improve the shape and design, and better maintain the characteristics of the hybrid scaffold, compared to the biodegradable scaffold made only by natural materials.[8–11,26,27]

Previous investigation of 3D fabricated porous scaffolds showed that the smooth surface and large pores cause these scaffolds to fail to favor cell residence, and render an adverse effect on the attachment of cellular and biological factors.[21,31] Multiple studies have been conducted to improve its biological performance using rather complicated and expensive techniques, including surface coating, scaffold etching, and microstructure adjusting, which may ease the cell adhesion but simultaneously decrease the mechanical strength.[31,32] Other attempts aimed to deliver heterologous cells and biologically active molecules into a 3D porous scaffold to build a hybrid scaffold. However, this may encounter crucial barriers in therapeutic translation, such as immunological rejection, pathogen transmission, potential tumorigenesis, and incompatibility with normal tissue.[42–45] In this study, the biochemical content of type II collagen, GAG, and DNA in Group A was significantly higher than in Group B. Similarly, the real-time PCR showed that the expression of type II collagen, GAG, and Sox9 in Group A was apparently higher than in Group B. As shown by histology and immunohistochemical assay, and by SEM observation, Group A had more cells and ECM accumulation than Group B throughout the experiment. These results showed that the composite construct in Group A had a significant improvement on chondrogenesis performance compared to Group B, and PCL-HA scaffolds can promote the chondrogenesis of MC following microfracture. From the results of this study, it was suspected that fibrin would remain in the scaffold during the initial culture, the aggregation of secreted ECM would promote marrow cell adhesion, and TGF-β3 would retain from cartilage induction medium. Since TGF-β3 is a potent stimulator of cartilage differentiation in stem cells, and BMSC-ECM contains proteins and growth factors of various structure and function, it's reasonable that Group A displayed better chondrogenesis performance than Group B.

From the SEM and live/dead confocal images of MC-PCL-HA scaffolds, we found that the pores of scaffolds were filled with fibrin, monocytes, and erythrocytes from MC at day 1. Meanwhile, the decreasing live/dead cell ratio observed at the first *in vitro* culture was suspected to be due to the obstruction of nutrient exchange, at pores, by large amounts of fibrin and erythrocytes. In the following culture, erythrocytes and fibrin were gradually eluted with mesenchymal stem cell proliferation, secreted ECM accumulation, and porous recanalization. This may have caused the red color to fade and the yellow color to deepen at the macrostructure observation. An increase in live/dead cell ratio was observed in MC-PCL-HA scaffolds at the 2 week *in vitro* culture time point. However, in BMSC-seeded PCL-HA scaffolds, gradual cell proliferation and secreted ECM accumulation were found over time, which may have caused the higher live/dead cell ratio and a lower cell/ECM ratio during culture, compared to Group A.

To reduce the boundary effect,[31,46] scaffolds were trimmed before *in vitro* culture and *in vivo* implantation. The performance of scaffolds with complex 3D structures would not be significantly affected with this physical restraint. Additionally, this study did not distinguish between different types of stem cells in bone marrow blood, and whether or not there are

multiple stem cells beside BMSCs that can also differentiate into chondrocytes in MC-PCL-HA scaffolds needs to be clarified by further research. Meanwhile, as an autologous procedure, MC may circumvent the barriers encountered in allograft procedures, including immune rejection, pathogen transmission, issues with packaging, storage, and shipping, and difficulties in clinical adoption. The performance of the MC-PCL-HA scaffold in autologous *in vivo* studies needs further investigation.

In conclusion, 3D porous MC-PCL-HA scaffolds showed significantly improved biological performance in inductive culture when compared to a conventional BMSC-seeded PCL-HA scaffold. Furthermore, its size was stable during *in vitro* and *in vivo* culture, which was superior to conventional biodegradable scaffolds. In this study, the MC proved to be a highly efficient, reliable, and a simple new method to improve the biological performance of PCL-HA scaffolds. This research provides a theoretical basis for future studies regarding MC-PCL-HA scaffolding.

## Acknowledgments

The authors thank Dr. Yijin Wang, Shanghai University, Shanghai, China for his assistance with the CAD and mechanical test. We are also grateful for the scientific and English editing assistance from Dr. Leo Zheng and Mr. Kevork Khadarian at the University of California, Los Angeles. Support was provided by the National Natural Science Foundation of China (81171745) and the Postgraduate Student Innovation Foundation of Jiangsu Province.

## Disclosure Statement

No competing financial interests exist.

## References

1. Buckwalter, J.A., and Mankin, H.J. Articular cartilage: degeneration and osteoarthritis, repair, regeneration, and transplantation. Instr Course Lect **47,** 487, 1998.
2. Gomez-Sanchez, C., Kowalczyk, T., Ruiz De Eguino, G., Lopez-Arraiza, A., Infante, A., Rodriguez, C.I., Kowalewski, T.A., Sarrionandia, M., and Aurrekoetxea, J. Electrospinning of poly(lactic acid)/polyhedral oligomeric silsesquioxane nanocomposites and their potential in chondrogenic tissue regeneration. J Biomater Sci Polym Ed **25,** 802, 2014.
3. Lutzner, J., Kasten, P., Gunther, K.P., and Kirschner, S. Surgical options for patients with osteoarthritis of the knee. Nat Rev Rheumatol **5,** 309, 2009.
4. Frappier, J., Stanish, W., Brittberg, M., Steinwachs, M., Crowe, L., Castelo, D., and Restrepo, A. Economic evaluation of BST-CarGel as an adjunct to microfracture vs microfracture alone in knee cartilage surgery. J Med Econ **17,** 266, 2014.
5. Wegener, B., Schrimpf, F.M., Bergschmidt, P., Pietschmann, M.F., Utzschneider, S., Milz, S., Jansson, V., and Müller, P.E. Cartilage regeneration by bone marrow cells-seeded scaffolds. J Biomed Mater Res A **95,** 735, 2010.
6. Lafantaisie-Favreau, C.H., Guzman-Morales, J., Sun, J., Chen, G., Harris, A., Smith, T.D., Carli, A., Henderson, J., Stanish, W.D., and Hoemann, C.D. Subchondral presolidified chitosan/blood implants elicit reproducible early osteochondral wound-repair responses including neutrophil and stromal cell chemotaxis, bone resorption and repair, enhanced repair tissue integration and delayed matrix deposition. BMC Musculoskelet Disord **14,** 27, 2013.
7. McCormick, F., Harris, J.D., Abrams, G.D., Frank, R., Gupta, A., Hussey, K., Wilson, H., Bach, B., Jr., and Cole, B. Trends in the surgical treatment of articular cartilage lesions in the United States: an analysis of a large private-payer database over a period of 8 years. Arthroscopy **30,** 222, 2014.
8. Wei, B., Jin, C., Xu, Y., Du, X., Yan, C., Tang, C., Ansari, M., and Wang, L. Chondrogenic differentiation of marrow clots after microfracture with BMSC-derived ECM scaffold in vitro. Tissue Eng Part A **20,** 2646, 2014.
9. Dai, L., He, Z., Zhang, X., Hu, X., Yuan, L., Qiang, M., Zhu, J., Shao, Z., Zhou, C., and Ao, Y. One-step repair for cartilage defects in a rabbit model: a technique combining the perforated decalcified cortical-cancellous bone matrix scaffold with microfracture. Am J Sports Med **42,** 583, 2014.
10. Steadman, J.R., Rodkey, W.G., and Briggs, K.K. Microfracture to treat full-thickness chondral defects: surgical technique, rehabilitation, and outcomes. J Knee Surg **15,** 170, 2002.
11. Stanish, W.D., McCormack, R., Forriol, F., Mohtadi, N., Pelet, S., Desnoyers, J., Restrepo, A., and Shive, M.S. Novel scaffold-based BST-CarGel treatment results in superior cartilage repair compared with microfracture in a randomized controlled trial. J Bone Joint Surg Am Vol **95,** 1640, 2013.
12. Mackie, E.J., Ahmed, Y.A., Tatarczuch, L., Chen, K.S., and Mirams, M. Endochondral ossification: how cartilage is converted into bone in the developing skeleton. Int J Biochem Cell Biol **40,** 46, 2008.
13. Zheng, R., Duan, H., Xue, J., Liu, Y., Feng, B., Zhao, S., Zhu, Y., Liu, Y., He, A., Zhang, W., Liu, W., Cao, Y., and Zhou, G. The influence of Gelatin/PCL ratio and 3-D construct shape of electrospun membranes on cartilage regeneration. Biomaterials **35,** 152, 2014.
14. Kaul, G., Cucchiarini, M., Remberger, K., Kohn, D., and Madry, H. Failed cartilage repair for early osteoarthritis defects: a biochemical, histological and immunohistochemical analysis of the repair tissue after treatment with marrow-stimulation techniques. Knee Surg Sports Traumatol Arthrosc **20,** 2315, 2012.
15. Rohner, D., Hutmacher, D.W., Cheng, T.K., Oberholzer, M., and Hammer, B. *In vivo* efficacy of bone-marrow-coated polycaprolactone scaffolds for the reconstruction of orbital defects in the pig. J Biomed Mate Res Part B Appl Biomater **66,** 574, 2003.
16. Carletti, E., Motta, A., and Migliaresi, C. Scaffolds for tissue engineering and 3D cell culture. Methods Mol Biol **695,** 17, 2011.
17. Hutmacher, D.W., Schantz, T., Zein, I., Ng, K.W., Teoh, S.H., and Tan, K.C. Mechanical properties and cell cultural response of polycaprolactone scaffolds designed and: fabricated via fused deposition modeling. J Biomed Mater Res **55,** 203, 2001.
18. Zein, I., Hutmacher, D.W., Tan, K.C., and Teoh, S.H. Fused deposition modeling of novel scaffold architectures for tissue engineering applications. Biomaterials **23,** 1169, 2002.
19. Zhu,G., Xu, Q., Qin, R., Yan, H., and Liang, G. Effect of y-radiation on crystallization of Polycaprolactone. Radiat Phys Chem **74,** 42, 2005.
20. Coombes, A.G., Rizzi, S.C., Williamson, M., Barralet, J.E., Downes, S., and Wallace, W.A. Precipitation casting of polycaprolactone for applications in tissue engineering and drug delivery. Biomaterials **25,** 315, 2004.
21. Schagemann, J.C., Chung, H.W., Mrosek, E.H., Stone, J.J., Fitzsimmons, J.S., O'Driscoll, S.W., and Reinholz, G.G. Poly-epsilon-caprolactone/gel hybrid scaffolds for cartilage tissue engineering. J Biomed Mater Res Part A **93,** 454, 2010.

22. Lou, T., Leung, M., Wang, X., Chang, J.Y., Tsao, C.T., Sham, J.G., Edmondson, D., and Zhang, M. Bi-layer scaffold of chitosan/PCL-nanofibrous mat and PLLA-microporous disc for skin tissue engineering. J Biomed Nanotechnol **10,** 1105, 2014.
23. Jin, C.Z., Park, S.R., Choi, B.H., Lee, K.Y., Kang, C.K., and Min, B.H. Human amniotic membrane as a delivery matrix for articular cartilage repair. Tissue Eng **13,** 693, 2007.
24. Tang, C., Jin, C., Du, X., Yan, C., Min, B.H., Xu, Y., and Wang, L. An autologous bone marrow mesenchymal stem cell-derived extracellular matrix scaffold applied with bone marrow stimulation for cartilage repair. Tissue Eng Part A **20,** 2455, 2014.
25. Tang, C., Xu, Y., Jin, C., Min, B.H., Li, Z., Pei, X., and Wang, L. Feasibility of autologous bone marrow mesenchymal stem cell-derived extracellular matrix scaffold for cartilage tissue engineering. Artif Organs **37,** E179, 2013.
26. Rai, B., Oest, M.E., Dupont, K.M., Ho, K.H., Teoh, S.H., and Guldberg, R.E. Combination of platelet-rich plasma with polycaprolactone-tricalcium phosphate scaffolds for segmental bone defect repair. J Biomed Mater Res Part A **81,** 888, 2007.
27. Milano, G., Sanna Passino, E., Deriu, L., Careddu, G., Manunta, L., Manunta, A., Saccomanno, M.F., and Fabbriciani, C. The effect of platelet rich plasma combined with microfractures on the treatment of chondral defects: an experimental study in a sheep model. Osteoarthritis Cartilage **18,** 971, 2010.
28. Yin, Z., Yang, X., Jiang, Y., Xing, L., Xu, Y., Lu, Y., Ding, P., Ma, J., Xu, Y., and Gui, J. Platelet-rich plasma combined with agarose as a bioactive scaffold to enhance cartilage repair: an *in vitro* study. J Biomater Appl **28,** 1039, 2014.
29. Christensen, B.B., Foldager, C.B., Hansen, O.M., Kristiansen, A.A., Le, D.Q., Nielsen, A.D., Nygaard, J.V., Bunger, C.E., and Lind, M. A novel nano-structured porous polycaprolactone scaffold improves hyaline cartilage repair in a rabbit model compared to a collagen type I/III scaffold: *in vitro* and *in vivo* studies. Knee Surg Sports Traumatol Arthrosc **20,** 1192, 2012.
30. Lee, C.H., Marion, N.W., Hollister, S., and Mao, J.J. Tissue formation and vascularization in anatomically shaped human joint condyle ectopically *in vivo*. Tissue Eng Part A **15,** 3923, 2009.
31. Lee, C.H., Cook, J.L., Mendelson, A., Moioli, E.K., Yao, H., and Mao, J.J. Regeneration of the articular surface of the rabbit synovial joint by cell homing: a proof of concept study. Lancet **376,** 440, 2010.
32. Min, B.H., Choi, W.H., Lee, Y.S., Park, S.R., Choi, B.H., Kim, Y.J., Jin, L.H., and Yoon, J.H. Effect of different bone marrow stimulation techniques (BSTs) on MSCs mobilization. J Orthop Res **31,** 1814, 2013.
33. Yao, Q., Wei, B., Guo, Y., Jin, C., Du, X., Yan, C., Yan, J., Hu, W., Xu, Y., Zhou, Z., Wang, Y., and Wang, L. Design, construction and mechanical testing of digital 3D anatomical data-based PCL-HA bone tissue engineering scaffold. J Mater Sci Mater Med **26**, 5360, 2015.
34. Li, L.H., Kommareddy, K.P., Pilz, C., Zhou, C.R., Fratzl, P., and Manjubala, I. *In vitro* bioactivity of bioresorbable porous polymeric scaffolds incorporating hydroxyapatite microspheres. Acta Biomater **6,** 2525, 2010.
35. Sun, H., Mei, L., Song, C., Cui, X., and Wang, P. The *in vivo* degradation, absorption and excretion of PCL-based implant. Biomaterials **27,** 1735, 2006.
36. Ramanath, H.S., Chua, C.K., Leong, K.F., and Shah, K.D. Melt flow behaviour of poly-epsilon-caprolactone in fused deposition modelling. J Mater Sci Mater Med **19,** 2541, 2008.
37. Breinan, H.A., Martin, S.D., Hsu, H.P., and Spector, M. Healing of canine articular cartilage defects treated with microfracture, a type-II collagen matrix, or cultured autologous chondrocytes. J Orthop Res **18,** 781, 2000.
38. Zantop, T., and Petersen, W. Arthroscopic implantation of a matrix to cover large chondral defect during microfracture. Arthroscopy **25,** 1354, 2009.
39. Li, W.J., Tuli, R., Huang, X., Laquerriere, P., and Tuan, R.S. Multilineage differentiation of human mesenchymal stem cells in a three-dimensional nanofibrous scaffold. Biomaterials **26,** 5158, 2005.
40. Rezgui, F., Swistek, M., Hiver, J.M., G'Sell, C., and Sadoun, T. Deformation and damage upon stretching of degradable polymers (PLA and PCL). Polymer **46,** 7370, 2005.
41. Labet, M., and Thielemans, W. Synthesis of polycaprolactone: a review. Chem Soc Rev **38,** 3484, 2009.
42. Yang, F., Wolke, J.G.C., and Jansen, J.A. Biomimetic calcium phosphate coating on electrospun poly (epsilon-caprolactone) scaffolds for bone tissue engineering. Chem Eng J **137,** 154, 2008.
43. Li, W.J., Tuli, R., Okafor, C., Derfoul, A., Danielson, K.G., Hall, D.J., and Tuan, R.S. A three-dimensional nanofibrous scaffold for cartilage tissue engineering using human mesenchymal stem cells. Biomaterials **26,** 599, 2005.
44. Zhang, Z.Y., Teoh, S.H., Chong, W.S., Foo, T.T., Chng, Y.C., Choolani, M., and Chan, J. A biaxial rotating bioreactor for the culture of fetal mesenchymal stem cells for bone tissue engineering. Biomaterials **30,** 2694, 2009.
45. Kuo, A.C., Rodrigo, J.J., Reddi, A.H., Curtiss, S., Grotkopp, E., and Chiu, M. Microfracture and bone morphogenetic protein 7 (BMP-7) synergistically stimulate articular cartilage repair. Osteoarthritis Cartilage **14,** 1126, 2006.
46. Fang, Z., Starly, B., and Sun, W. Computer-aided characterization for effective mechanical properties of porous tissue scaffolds. Comput Aid Des **37,** 65, 2005.

Address correspondence to:
*Liming Wang, MD*
*Department of Orthopaedic Surgery*
*Nanjing First Hospital*
*Nanjing Medical University*
*Nanjing 210006*
*Jiangsu Province*
*China*

*E-mail:* limingwang99@hotmail.com

*Xinli Zhang, MD, PhD*
*Dental and Craniofacial Research Institute*
*University of California, Los Angeles (UCLA)*
*10833 Le Conte Ave., CHS 73-060*
*Los Angeles, CA 90095-1668*

*E-mail:* xzhang@dentistry.ucla.edu

*Xiuwu Bian, MD, PhD*
*Institute of Pathology and Southwest Cancer Center*
*Southwest Hospital*
*Third Military Medical University*
*Chongqing 400038*
*China*

*E-mail:* bianxiuwu@263.net

*Received: May 14, 2014*
*Accepted: December 16, 2014*
*Online Publication Date: March 19, 2015*